Sound propagation in regions of variable oceanography – a summary of student work at NTNU

Ulf Kristiansen

Norwegian Defence Research Establishment (FFI)

15 April 2010

FFI-rapport 2010/00812

1062

P: ISBN 978-82-464-1776-9
E: ISBN 978-82-464-1777-6

Keywords

Kystnær lydforplantning

Strålegang

Avstandsavhengig oseanografi

Approved by

Atle Omundsen	Project Manager
Jan Erik Torp	Director

English summary

Two ray tracing programs, Lybin and Ray5, have been used in student projects at NTNU to study wave propagation in range dependent environments. For a given set of sound speed profiles obtained during a FFI measuring campaign, the programs were found to give similar ray trace diagrams. The report addresses the necessary number of constant sound speed profile range blocks that are needed when using Lybin for range dependent propagation and presents some rules of thumb. Sound propagation in some range dependent bench mark scenarios are also presented. These are: Sound propagation through an internal hydrodynamic wave, sound propagation in the region of a hot core vortex, and sound propagation in the region of an internal wave having split up into a row of individual solitons.

Samandrag

To strålegangsprogram, Lybin og Ray5, har vært brukt i studentprosjekter ved NTNU til å studere lydutbredelse i områder med avstandsavhengig oseanografi. For et gitt sett med lydfartprofiler målt under en av FFIs målekampanjer gav begge programmene likt utseende strålediagram. I rapporten blir det diskutert hvor mange blokkinndelinger som er nødvendige ved bruk av Lybin og det blir presentert noen tommelfingerregler.

Lydutbredelse i noen ”bench mark” situasjoner som er definert for avstandsavhengig oseanografi tilfelle er også presentert i rapporten. Disse er: Lydutbredelse gjennom en intern hydrodynamisk bølge, lydutbredelse i et område som inneholder en varm kjerne hvirvel og lydutbredelse i et område der en intern bølge er delt opp i en rekke individuelle solitære bølger.

Contents

1	**Executive Summary**	**7**
2	**Introduction**	**8**
3	**Comparing Lybin and Ray5 for a measured sound speed field**	**9**
3.1	The sound speed field	9
3.2	Comparing Ray5 and Lybin ray diagrams on raw data	11
3.3	Comparing Ray5 and Lybin ray diagrams on smoothed data	11
3.4	Convergence study	11
3.4.1	Measured sound speeds	11
3.4.2	Feature modeling	15
4	**Study of sound interacting with an internal hydrodynamic wave**	**18**
5	**Study of sound interacting with a warm core eddy**	**23**
6	**A soliton environment**	**25**
7	**Conclusions**	**32**
	Bibliography	**33**

1 Executive Summary

This report is a summary of some student projects done at The Norwegian University of Science and Technology (NTNU) in collaboration with the Norwegian Defence Research Establishment (FFI). The projects concern acoustic propagation in waters having range dependent oceanography, that is, situations where the sound speed profiles change in the horizontal direction. Two ray tracing programs have been used to study several scenarios, Lybin and Ray5. In a first study, designed to compare the results from the two programs, they were used to study propagating sound rays in a domain where sound speeds had been measured at 20 stations for a 30km stretch in an earlier FFI measuring campaign. Ray5 is a so called direct integration program and directly suited to include range dependent environments in the calculations, while Lybin must divide the environment into blocks of constant speed profiles covering specified ranges. After suitable data smoothing, the ray traces became very similar. This gives confidence in using Lybin for range dependent environments.

The number of blocks needed to model a range dependent environment was tested for two scenarios, the measured sound speed environment mentioned above and a ”feature” modeled one where two volumes of constant, but different, speed profiles are joined by a transition zone of given width and angular inclination. It was found that for the measurement campaign scenario, the number of blocks needed correspond to the number of independent speed profile measurements, while for the ”feature” modeled scenario, the block width should at least be as small as the width of the transition region.

The Ray5 program was further used to study sound propagation in somewhat idealized range dependent situations: 1) wave propagation through an internal oceanographic wave, 2) long range propagation in the region of a hot center vortex, and 3) sound propagation in the region of an internal wave broken up into 4 solitary sound speed disturbances.

The ray diagrams and corresponding transmission loss calculations showed that for sound transmission through an internal wave, the rays would focus on regions below and close to the throughs of the internal wave. Strong sound pressure fluctuations are therefore expected in these regions for short range changes.

A benchmark simulation of long range propagation in the region of a hot-core vortex, showed that Ray5 would give results qualitatively close to results obtained by other methods.

In a simulation of an upper layer transmission channel it was shown that the larger part of the acoustic energy was lost from the channel in the case where a number of solitons were present.

2 Introduction

Range dependent oceanography will in some cases play an important role for underwater sound propagation. This is also the case in Norwegian coastal waters where range dependency is created by for instance the water circulations caused by the the northgoing coastal stream meeting the southgoing atlantic one. Measurement campains by the FFI clearly show such range dependancies. Student projects at the NTNU have studied such phenomena using two available program packages developed and maintained by the FFI, Ray5 and Lybin. The results are described in two master thesises and student reports at the NTNU. The purpose of the present report is to summarize and add to these results. For more detailed discussions on details of this research as well as the necessary computer coding for special calculations and preparation of data files, the reader is asked to see the reports referenced in the attached bibliography.

Most underwater sound propagation models based on ray-tracing do not consider range dependent oceanography. An exception to this is the Lybin program where range dependency might be included by considering depth sound speed profiles characteristic for given range blocks. Another exception is the Ray5 program developed by Trond Jenserud at the FFI which uses direct integration in a sound speed field given analytically or by interpolation from measured data.

The two programs are quite different inasmuch as Lybin is a fast operational tool intended for use by for instance The Royal Norwegian Navy, while Ray5 is more a research tool. Calculations by Ray5 are orders of magnitude slower than Lybin and lacks the surrounding structure, *i.e.* the graphical user interface, and flexible pre- and post processing capabilities. Recent developments have however added possibilities of eigenray calculations and routines to calculate coherent and incoherent transmission losses. Ray5 basically calculates the ray paths, it is however considered more exact than Lybin in ray path calculations as it does not need the block division of the sound speed field (or the assumption of linearly varying speed segments in the depth direction), but integrates for small steps through the entire field. To do this, Ray5 starts by defining a ray direction and draws a short ray segment in this direction. To continue, the program needs information of sound speed and sound speed derivatives. For an analytically described field this is simple, while for a measured one not only the velocity components, but also their derivatives, must be found by interpolation.

The purpose of this report is to give an overview of student projects done at NTNU where the object has partly been to use and compare these two programs in scenarios involving range dependancy.

The questions sought answered by these projects have been:

- For a given sound velocity field, how well do Lybin and Ray5 results compare? This was of interest for the validation of range dependent Lybin. This is reported in section 3.2 of the report.
- Using Lybin for different sound speed fields, how many range blocks are needed for convergence of the transmission loss results. This is reported in section 3.3 of the report for sets of

measured and analytically derived velocity fields.

This is followed by three sections giving results for different range dependent scenarios, all investigated with the help of Ray5.

- Section 4 presents a study of ray tracing in a well described range dependent environment, a sinusoidally varying thermocline.
- Section 5 illustrates the need for range dependent calculations in a hot vortex core scenario suggested in the textbook by Jensen et al. [6].
- In section 6 one of the benchmark problems suggested in SWAM99 is treated, sound transmission through a set of 5 solitons defined at the interface between an upper mixing layer and a region of "decreasing with depth" sound speeds.

The above scenarios are all considered to be deterministic. Random fluctuations that occur in real life situations are not included.

3 Comparing Lybin and Ray5 for a measured sound speed field

This was investigated by Håvar Slåttrem Olsen and Even Martin Grytå in their Masters and 5th year projects [8], [4], and [9]. The basic feature of the two programs is the tracing of acoustic rays. This forms the basis of further evaluation, as transmission losses, reverberation, etc. It was therefore of interest to compare ray tracing diagrams calculated by Lybin and Ray5. Lybin calculates the ray paths as joined circular segments. This can be done as the vertical sound speed profiles are assumed to consist of linear segments. Ray5 uses a direct integration technique where the rays are advanced a short distance at the time and its direction determined by local sound speed gradients. See [6] for an outline of the different methods. There is a considerable calculation time difference between the two methods, Lybin only uses a fraction of the time required for Ray5 to calculate the same scenario. To calculate range dependent environments, Lybin users must divide the water volume into horizontal "blocks". Within each block is used a constant sound speed profile. Sound rays traverse the boundaries by retaining their directions across the boundaries. Ray5 is expected to calculate the range dependent ray paths more correctly than Lybin as it directs the rays by local information. It is however dependent on accurate information on not only the local sound speed, but also the sound speed derivatives.

3.1 The sound speed field

The sound speeds were measured during a FFI measurements campaign off the Norwegian Southwestern coast. Figure 3.1 shows in a sketch how the coastal and Atlantic streams meet in this region,

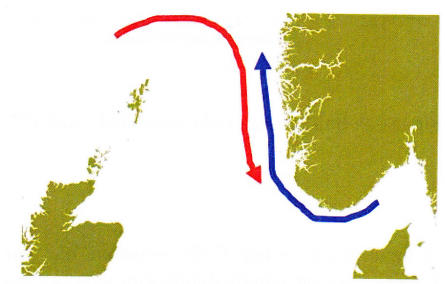

Figure 3.1: Sketch showing coastal and atlantic streams meeting off norwegian south west coast.

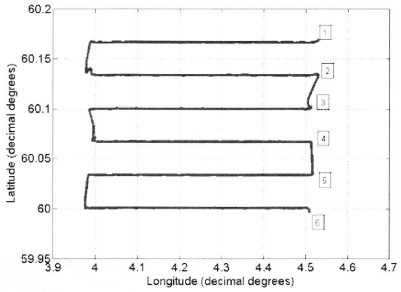

Figure 3.2: run lines for towed CTD.

and figure 3.2 the traces traversed by a ship towing a sound speed measuring device, a CTD (Conductivity Temperature Depth) sensor logging data at a frequency of 1Hz. The data were obtained by moving the ship along 6 east-west or west-east lines, each of 30km range. The distance between each line was about 3,7km. The maximum measuring depth was about 180m. The towing device does not descend and go up again along perfect vertical lines, but follows a ”sinusoidal” pattern as shown in figure 3.3, measuring speed and position data continuously. The data obtained along the sinusoidal curves were interpolated for each line to about 20 vertical columns of data. Figure 3.3 shows 12 dives giving 24 such columns over a range of 30 km. The data were further interpolated along and between each vertical column and appear in files giving sound speed values for every 10 m in the horizontal and 1 m in the depth direction. In [9] Håvar Olsen presents ray traces from all the 6 measuring lines. Results using data from one of these, line 3, are presented in the following.

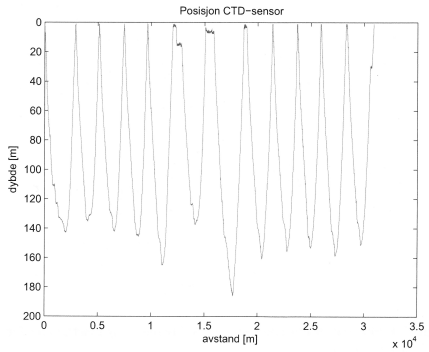

Figure 3.3: Motion of CTD sensor, vertical and horizontal axes show depth and range in m. Illustration for run 1.

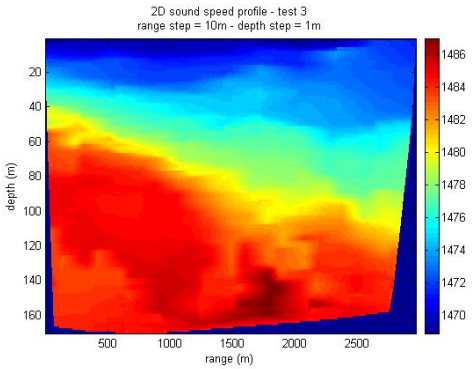

Figure 3.4: Sound speed data from run 3.

3.2 Comparing Ray5 and Lybin ray diagrams on raw data

Figure 3.5 shows raypaths calculated by the two methods for a scenario given by the measurement campaign shown in figure 3.4. A 10km stretch was chosen. Even though the rough features are similar, odd ray behavior is seen in the Ray5 diagram. This is caused by the fact that the data are not continuos but given as values in a 3000 by 180 matrix (for the complete region), generated by linear interpolations within the original measured data set. Further interpolation was used to estimate derivatives. The derivatives are found by finite difference approximations.There are points within such an interpolated field which do not give precise derivatives and hence the sometimes odd ray behavior. Also, as rectangularly defined region seen in the plots do not have full coverage in the measurements data, the "blue regions" of figure 3.4 are filled in by extrapolation. Normally by assuming the sound speed distribution along a vertical or horizontal line to continue into the unknown region by the last value of the investigated region [1]. The chosen 10km stretch was taken from the middle of the data set to avoid large portions of extrapolated data.

Lybin on the other hand does not need such derivatives and gives a much smoother plot. The lower of the fig 3.5 plots shows a Lybin version of the same scenario. The 10 km stretch was divided in 25 blocks, each given a vertical sound speed distribution. Each block hence covers 400m of the 10km stretch.

3.3 Comparing Ray5 and Lybin ray diagrams on smoothed data

Better results are obtained if smoothing the data. This was done by applying a two dimensional Gaussian spatial filter. Every value in the 3000 by 180 value matrix is replaced by a new mean value based on the point value itself and its eight neighbors. The point itself is weighted by 1, its vertical and horizontal neighbors by e^{μ}, and the diagonal neighbors by $e^{2\mu}$. μ was set to unity for most of the generated plots. Special attention had to be taken for the edge and corner values of the matrix. For more details about the technique see [2]. It was found that applying the filter only once had a small effect on the results with the chosen settings. The filter had to be applied a number of times, 50 in the results shown below, for the Lybin and Ray5 results to closely agree. From a comparison of the Lybin plots in 3.5 and 3.6, we also notice that running the dataset 50 times through the filter has only a small influence on the Lybin model results.

3.4 Convergence study

3.4.1 Measured sound speeds

As Lybin works with range 'blocks' of constant vertical velocity profiles it was of interest to investigate how many blocks were needed for a convergence was seen in the results. Apart from the

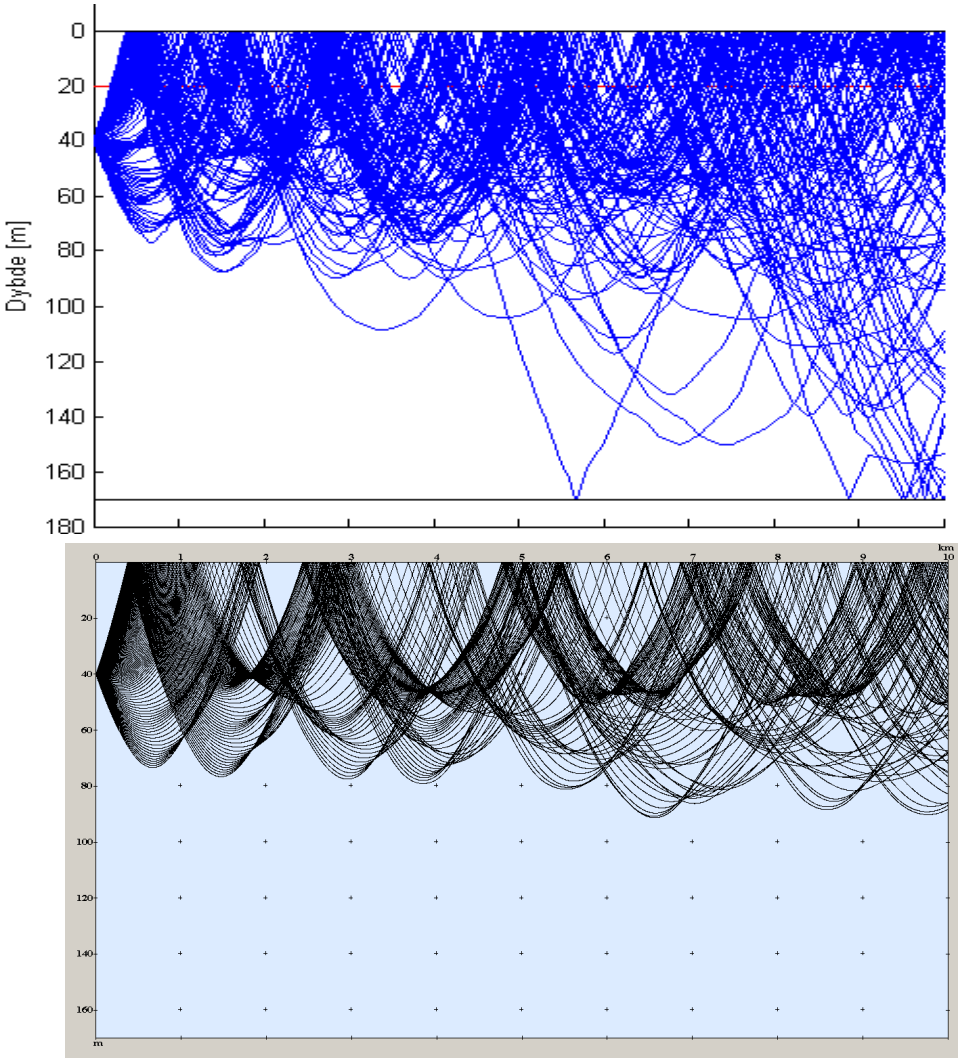

Figure 3.5: Raypaths calculated for a 10km stretch of line 3 of figure 3.2 (both plots use the same 10km range). Upper plot shows results produced by Ray5, lower plot shows results by Lybin using 25 blocks of constant sound speed profiles. For both plots the source depth is 40m, the vertical axis shows depth in m and the horizontal is marked from 0 to 10 km.

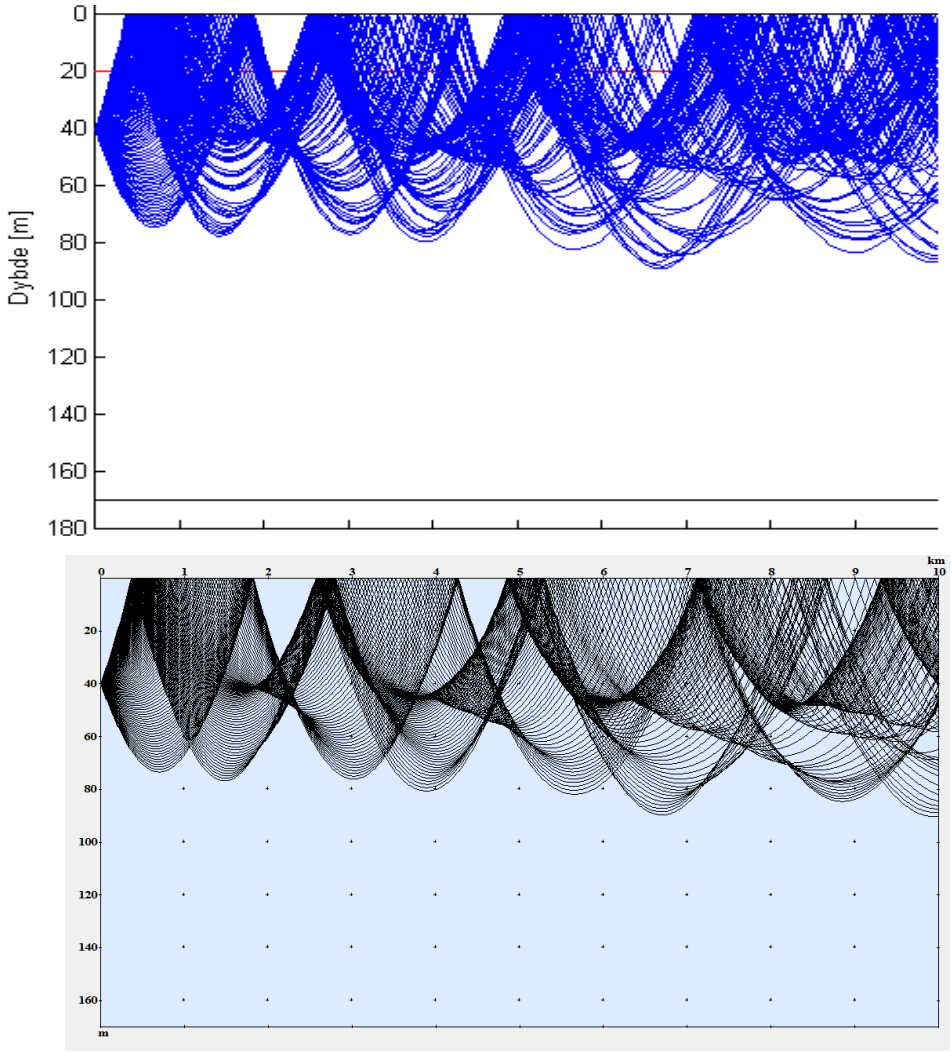

Figure 3.6: The same situation as in the previous figure, see legend 3.5. The measured data set has been run through a smoothing filter 50 times.

range dependent blocks, Lybin uses a set of cells in the vertical and horizontal directions for its basic calculations. For transmission loss calculations, Lybin estimates the transmission loss for each individual cell. An average transmission loss to be used in convergence studies can therefore be defined as the sum of all individual cell transmission losses divided by the number of cells.

The transmission loss (TL) matrix is given as:

$$TL(r,z) = \begin{pmatrix} TL_{11} & TL_{12} & \cdots & TL_{1n} \\ TL_{21} & TL_{22} & \cdots & TL_{2n} \\ \cdots & \cdots & \cdots & \cdots \\ TL_{m1} & TL_{m2} & \cdots & TL_{mn} \end{pmatrix},$$

where the subscripts indicate the cell number, ($M \cdot N$ cells).

We further used a function, C to calculate the average change in transmission loss for two different block divisions.

$$C = \frac{1}{M \cdot N} \sum_m \sum_n \left(TL^1_{mn} - TL^2_{mn} \right)^2,$$

where the superscripts 1 and 2 refer to two different block divisions. In the following graphs we always compare the averaged transmission loss for different numbers of blocks with a constant profile (single block) for the whole range.

The blue line in figure 3.7 is drawn for a linear interpolation between the original 24 measured CTD positions, and the red for a spline type of interpolation. The results show that although the curves converge to slightly different values, the number of blocks for convergence is about the same, *i.e.* around 24.

It was concluded that if a certain number of vertical CTD lines are obtained from a sea trail and intermediate lines are mere interpolations between these, a finer block division will not give a better result. The necessary number of blocks is given by the set of independent CTD lines from the sea trail.

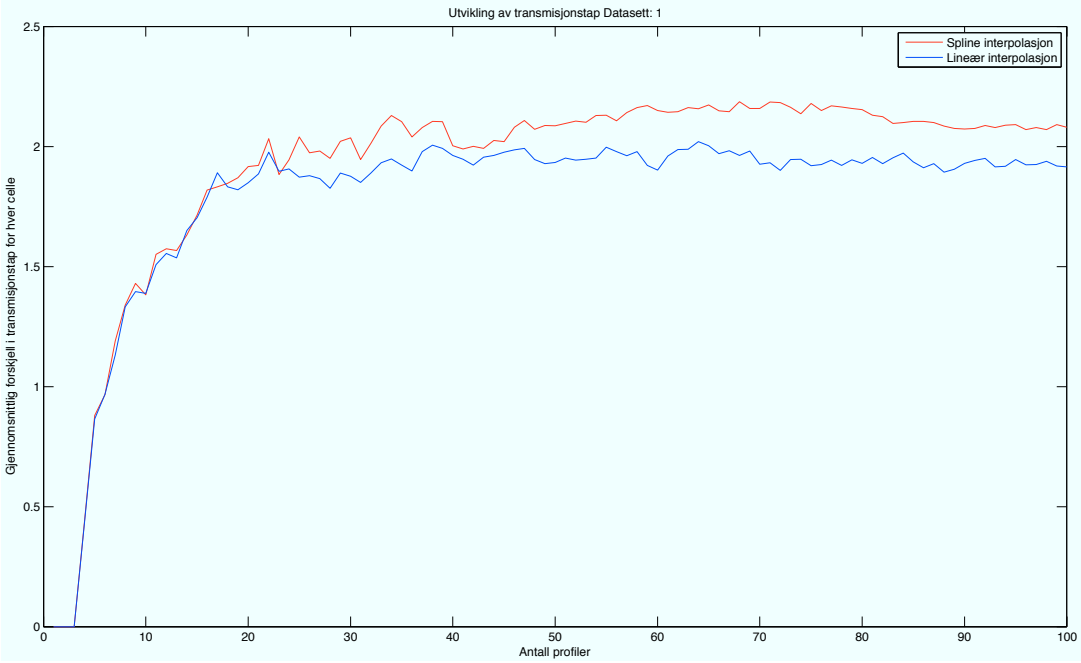

Figure 3.7: Convergence diagrams for the measured sound speed field. Blue line for linearly interpolated data, red line for spline interpolated data. The curves show averaged transmission loss for a given number of blocks compared to the averaged transmission loss using one block only vs. number of range blocks, values in [dB]. Diagram shows data up to 100 range blocks.

3.4.2 Feature modeling

Feature modeling is a method which can be used to join the oceanographic properties, including sound speed profiles, of for example two water volumes. A good reference is found in the paper by A. Gangopadhyay and A.R. Robinson [3]. Jan-Kristian Jensen of the FFI is currently writing a doctoral thesis on the subject. Figure 3.8 shows two speed profiles of the Munk type characterizing two volumes of water. They are joined by a transition zone illustrated in figure 3.9. For simplicity, the domain is considered 10km long and 135m deep. The transition zone can be at an angle with respect to the horizontal, and has a smooth $\tanh$ type of variation from one region to the other. The width is also a parameter of the transition zone. A detailed description of the method applied to the data presented in this section is given in [4]

Figure 3.11 shows a Lybin based ray plot for the feature modeled scenario. The sound source is placed at 40m depth. Notice that the repetitive structure of the diagram changes as the sound propagates in the two different water volumes.

Also in this case we investigated for convergence as function of number of blocks in the horizontal direction. Figure 3.12 shows the sound speeds at 20m depth. The transition zone at this depth is

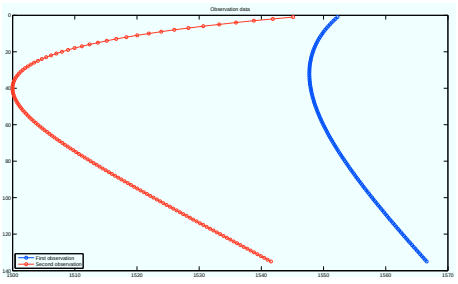

Figure 3.8: Speed profiles of two adjoining water volumes, vertical axis shows depth from 0 to 140m while horizontal axis is marked from 1500$\,m/s$ to 1570$\,m/s$.

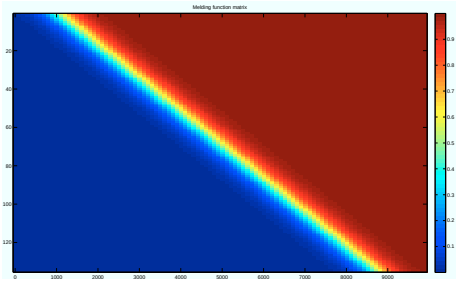

Figure 3.9: Transition region between two water volumes, vertical axis shows depth from 0 to 140$\,m$, and horizontal axis is marked between ranges 0 and 10$\,km$.

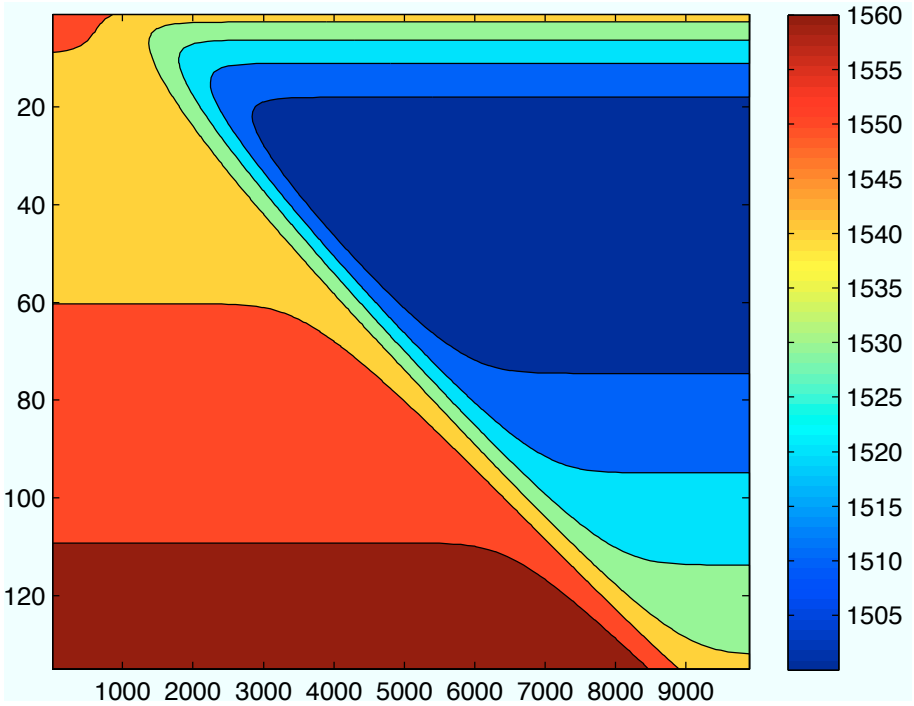

Figure 3.10: Sound speed distribution based on information in the two previous figures. Vertical axis shows depth in m, and horizontal axis range in m.

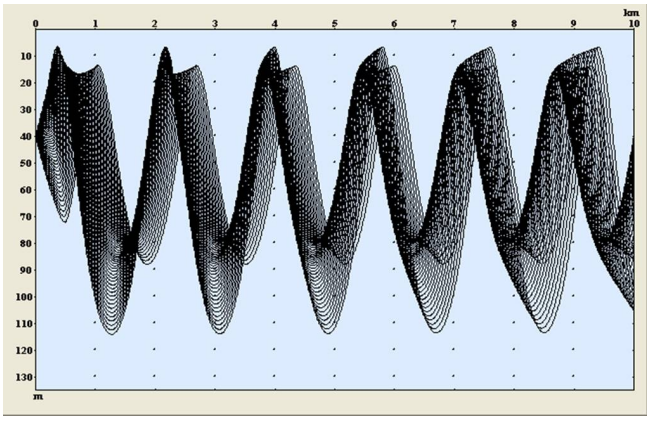

Figure 3.11: Plot of rays from source at 40m depth for sound speed distribution given in figure 3.10, depth and range as in figure 3.10.

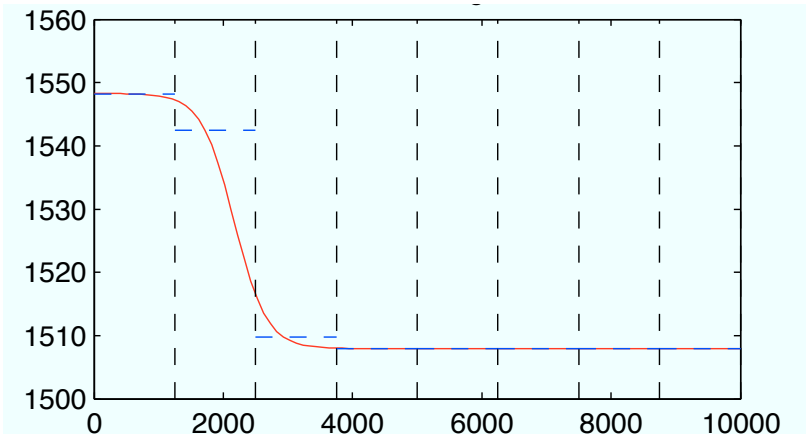

Figure 3.12: Sound speed values at 20m depth as function of range. Vertical axis shows sound speed in m/s and horizontal axis range from 0 to 10000 m. Eight range block divisions are indicated.

clearly visible. Also marked are the division lines for a 8 speed block division. It is seen that for 8 divisions, a block closely correspond to the width of the transition region. Note that the transition will take place at different ranges for different depths. A convergence plot for this situation is shown in figure 3.13. The plot shows convergence after 8 divisions, indicating that little more is gained after the block witdh has been reduced to the transition width.

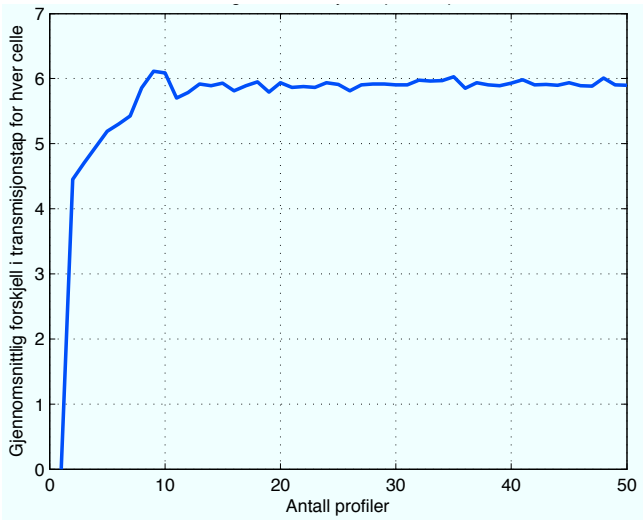

Figure 3.13: Convergence diagram for the feature modeled sound speed field. The curve show averaged transmission loss for a given number of blocks compared to the averaged transmission loss using one block only vs. number of range blocks, values in [dB]. Diagram shows data up to 50 range blocks.

4 Study of sound interacting with an internal hydrodynamic wave

Several authors have treated the problem of sound transmission through an internal hydrodynamic wave in the ocean. Such waves are often occurring in the upper 100 - 300m of the world's oceans, and often represent thermoclines, that is, narrow water layers of rapidly changing temperatures. Sound transmission through a thermocline might be strongly affected by the thermocline curling up into a wave,[5]. Owen S. Lee measured an internal wave off the coast of San Diego in California, [7] which has become a benchmark test for acoustic investigations. The two figures below show the scenario. The first sketch illustrates a flat and a wavy thermocline. Owen assumed the upper layer to be of constant sound speed, a rapid sound speed lowering in the layer, and a slow decrease below the thermocline. Remember that the distances considered are relatively short. The second picture, figure 4.2, shows the actual measurements done by Lee. Length measures are in feet, and temperatures in degrees Fahrenheit. Marie Darrieus (NTNU) investigated the scenario further using the Ray5 ray tracing program, [1].

The Ray5 program is especially well suited for ray tracing calculations in acoustic fields described analytically. It needs the sound speed values, their spatial derivatives and double derivatives at all possible points within the field. Hence, if these values can be given analytically as functions of the oceanographic and bathymetric parameters, no interpolation is necessary and the program reduces its computing time. The thermocline example given in this section and the soliton example in section 6 are examples of analytically described scenarios.

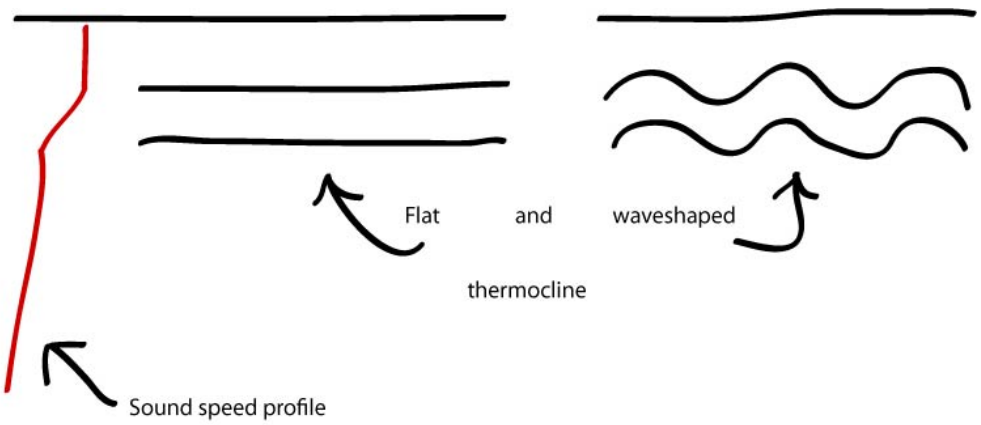

Figure 4.1: Sketch showing a flat thermocline and one in the form of an internal wave.

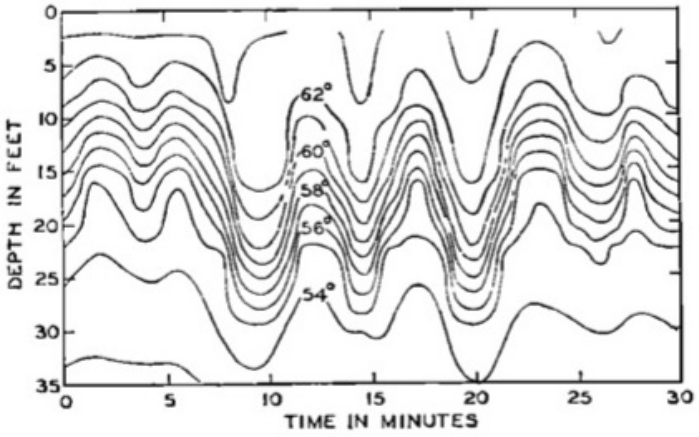

Figure 4.2: Example of a series of internal waves which were observed in 60 ft of water off the coast at San Diego California. Isotherms are shown in 1° *F intervals. Figure taken from [7].*

With the sound speed in the upper layer set to 1511.8 m/s, the three layer model was idealized by assuming the thermocline to be limited by z_1 and z_2 given by the equations:

$$\begin{aligned} 0 \quad &\leq z \quad \leq z_1(r), \qquad \partial c/\partial z = 0 \\ z_1(r) \quad &\leq z \quad \leq z_2(r), \qquad \partial c/\partial z = -4.8 \\ z_2(r) \quad &\leq z \quad \leq 100, \qquad \partial c/\partial z = -0.6 \end{aligned} \tag{4.1}$$

where:

$$\begin{aligned} z_1(r) &= 9.14 - 2.44sin(2\pi r/91.44) \\ z_2(r) &= 12.19 - 2.74sin(2\pi r/91.44) \end{aligned} \tag{4.2}$$

In the equations above, c, z, and r designate sound speed, depth, and horizontal range respectively. The distances z and r must be given in m.

Figures 4.3 and 4.4 show a ray-fan emitting rays between +/- 8 degrees with the horizontal. The source is situated at 3.048m depth and emits rays at 0.25 degree intervals, a total of 64 rays are therefore emitted. It is easily seen that the thermocline has an influence on the rays. The flat thermocline merely bends the rays as they enter, while the sinusoidal formation also seem to group the rays. This is more easily seen in figure 4.5 which is a zoom of part of figure 4.4. It is seen that the downward part of the sinusoidal layer collects rays and consequently focuses acoustic energy in a region below the throughs. Marie Darrieus first quantified this focusing effect by counting the number of rays passing "bins" of equal length along the 19m depth receiver line. From figures 4.6 and 4.7 it is seen that the flat thermocline has a more uniform falloff in number of rays passing a bin than in the sinusoidal case.

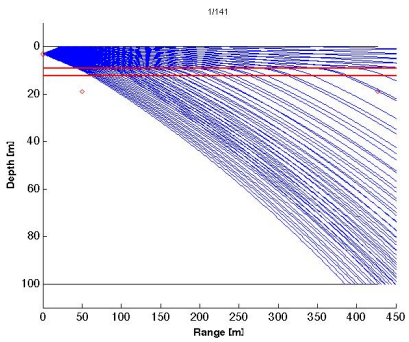

Figure 4.3: Rays through flat thermocline.

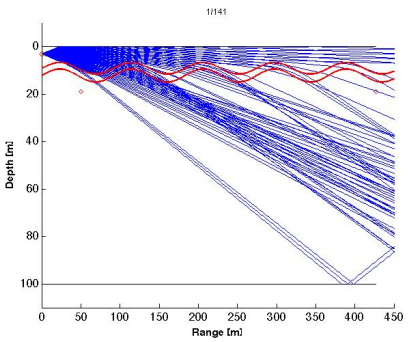

Figure 4.4: Rays through sinusoidal thermocline.

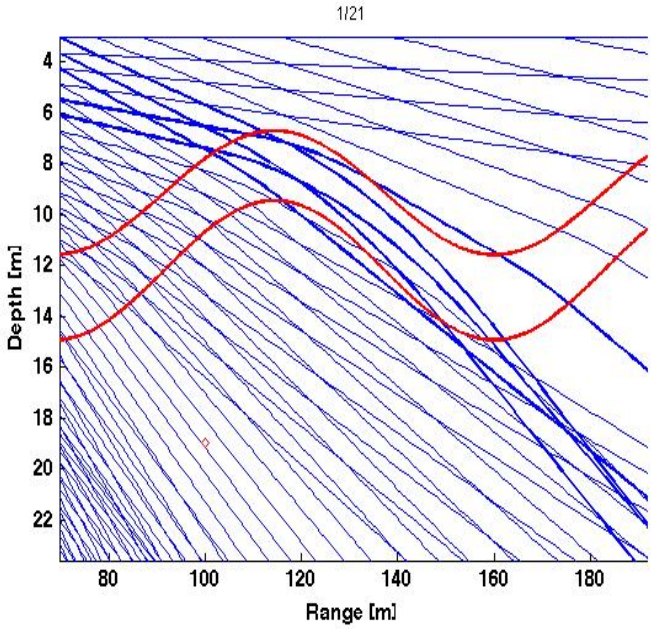

Figure 4.5: Zoom of previous slide.

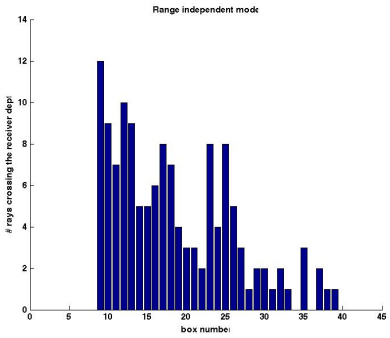

Figure 4.6:
For the range independent thermocline. Number of rays passing 10m long bins at 19m depth. 134 rays emitted between $\pm 10^{\circ}$.

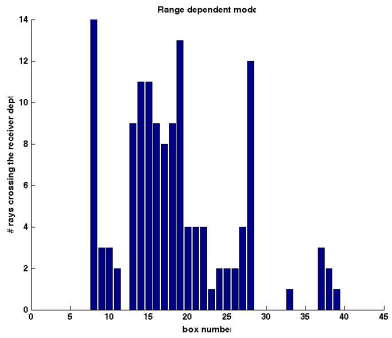

Figure 4.7:
For the range dependent thermocline. Number of rays passing 10m long bins at 19m depth. 134 rays emitted between $\pm 10^{\circ}$.

Further developments in Ray5 has made it possible to calculate so-called eigenrays, or rays connecting the source point with a given receiver. This allows phase information to be retained for a given frequency so that coherent pressure values can be summed for the rays arriving at the receiver. The actual pressure values for the individual rays are calculated by assuming the pressure distribution in the direction normal to the ray to have a Gaussian behavior (Gaussian beams) [10]. It is also possible to calculate the incoherent (based on energy and not respecting the different phases of the

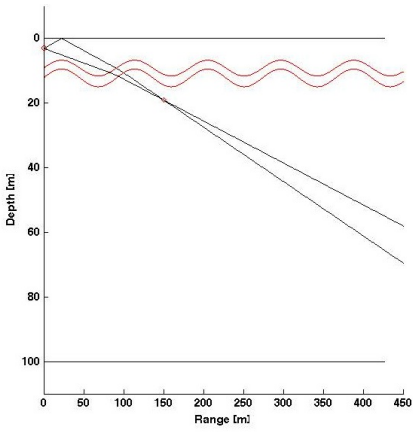

Figure 4.8: Eigenbeams arriving at receiver location 150m.

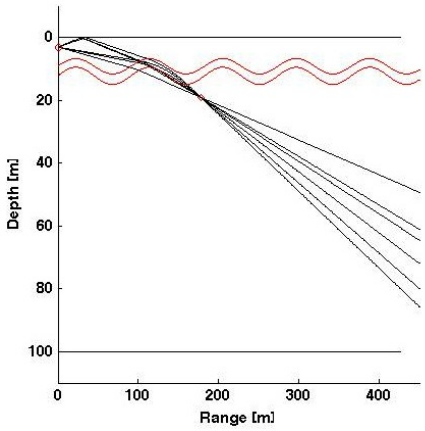

Figure 4.9: Eigenbeams arriving at location 177.5m.

arriving sound signals) sound levels.

The two figures above illustrate eigenbeams arriving at two different receiver locations, one away from the focusing area and one in the middle of it. The eigenbeams are sought by first defining a narrow ray fan, and thereafter look for eigenbeams within this fan. As only one beam is sought for each fan, they have to be defined reasonably narrow. Figure 4.8 shows the arrival of a direct ray, only refracted by the thermocline and the lower water volume., and one ray first having been reflected from the sea surface. Figure 4.9 shows a total of 6 rays arriving at the location. Five of the rays are seen to be strongly influenced by the downward slope of the thermocline. For locations where many eigenrays arrive, one might expect a build up of energy when assuming incoherent addition, and sometimes (depending on frequency) strong fluctuations in the coherent case.

The three sets of figures below, 4.10-4.11, 4.12-4.13, and 4.14-4.15 show the Transmission Loss (TL) vs. range for three different frequencies for the two thermocline configurations. The frequencies are 100, 1000, and 10000Hz. Both coherent (black line) and incoherent (red line) Transmission Losses are plotted. The incoherent TL is independent of frequency and is seen to fall smoothly in the flat thermocline case except for a jump at around 40m, where the sound level, which for smaller ranges was caused by a single beam arrival, now is composed by two. The second being a reflection from the water surface, which adds to the level in the incoherent case. The coherent calculation is seen to differ from the incoherent one and especially at the low frequency. This is due to the water surface reflection now adds to the direct with a phase shift close to π. Also here the levels are high in the focusing regions, but oscillate due to constructive/destructive interference between the many incoming rays in this region. The mean levels of the coherent/incoherent calculations are fairly close for the highest frequency, but also here we find high peaks in the focusing regions.

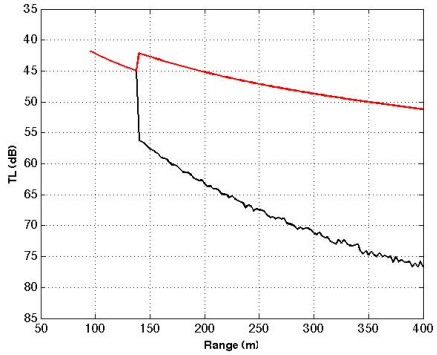

Figure 4.10: TL 100Hz, straight thermocline.

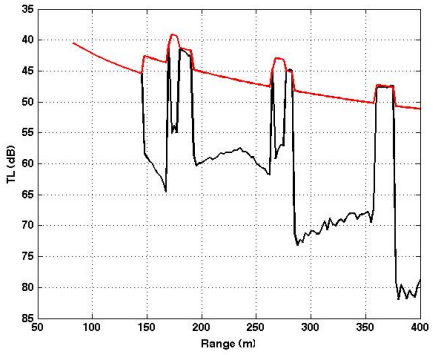

Figure 4.11: TL 100Hz, sinusoidal thermocline.

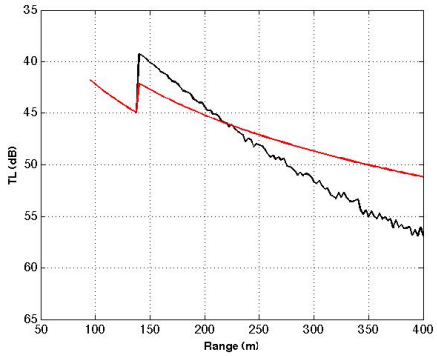

Figure 4.12: TL 1000Hz

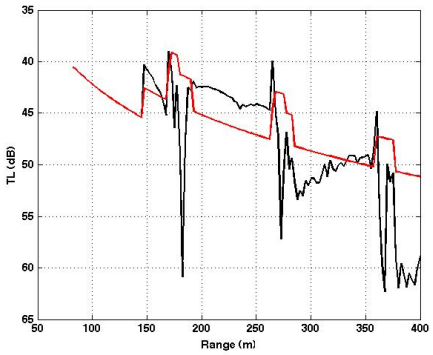

Figure 4.13: TL 1000Hz

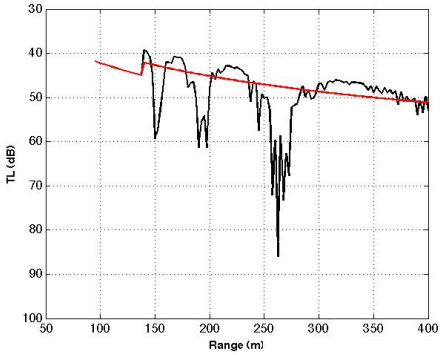

Figure 4.14: TL 10000Hz

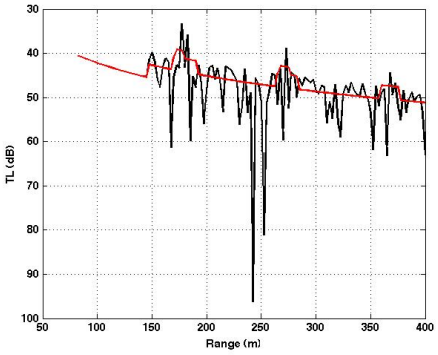

Figure 4.15: TL 10000Hz

5 Study of sound interacting with a warm core eddy

The example is taken from the book by Jensen et al. [6]. We consider a flat-bottom problem involving a warm-core eddy. The eddy is centered at zero range in this axi-symmetric situation. The

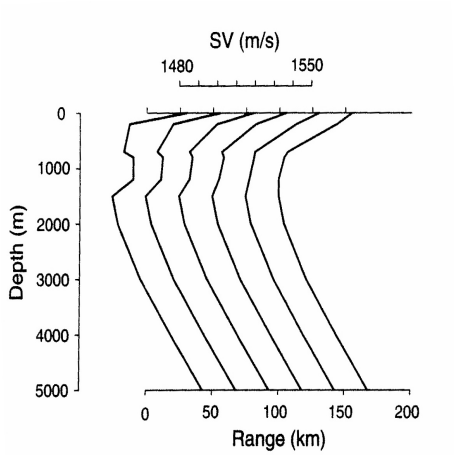

Figure 5.1: Sound speed profiles through the eddy, from [6]

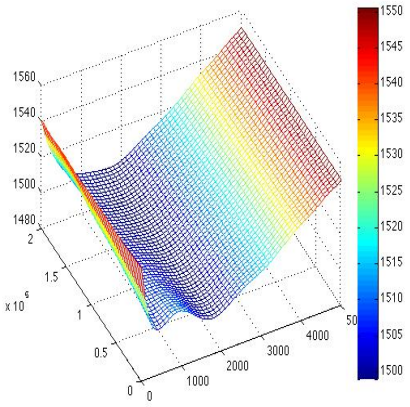

Figure 5.2: 2D polynomial interpolation of the sound speed profiles. Axes show depth, range and sound speed.

propagation is out to 200km, and the depth is 5000m. One of the purposes of the study was to see if a range dependent situation described by a given number of vertical profiles could be entered as input data to Ray5 via a 2 dimensional polynomial interpolation. The figure below show the profiles given as figure 5.17 in [6]. The data were interpolated to a finer grid and represented by a 12th order polynomial 2 dimensional fit. The polynomial fit is shown as figure 5.2 below.

The source is situated at 300m depth. The hot core eddy is located at 1000m depth and the locally high sound speed caused by the hot core is easily seen for the first profiles. The vortex is local and it's influence on the sound speeds is not seen after about 100km.

Figure 5.3 below shows a range independent situation where only the first depth profile is used for the whole stretch. It is seen that rays propagate in two channels. A major described by the Munk type profile not much influenced by the local maximum, and an upper channel bounded by the water surface and the local maximum. Figure 5.4 shows the range dependent situation. The upper channel is active up to a certain distance, beyond which the channeled energy is transferred to the central region. The result is in accordance with what is presented in [6] using a very different technique.

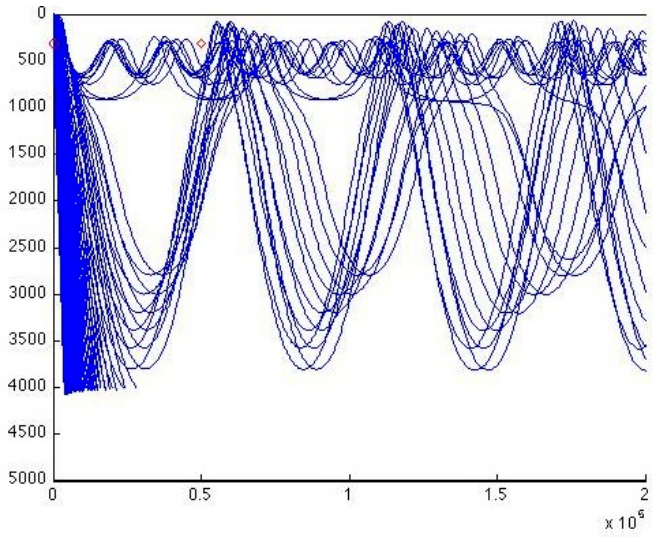

Figure 5.3: Ray diagram for a constant sound speed distribution given by the one through the vortex (first profile of figure 5.1), ray fan $\pm 45°$, sourcedepth 300m. Water depth and range: 5000m and 200km.

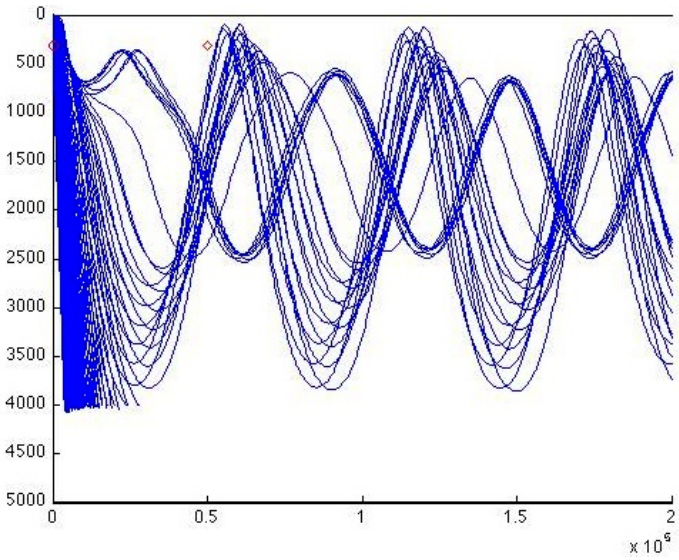

Figure 5.4: Ray diagram for range dependent sound speed distribution given by figure 5.2, ray fan $\pm 45°$, sourcedepth 300m. Water depth and range: 5000m and 200km.

6 A soliton environment

The SWAM99 workshop was held in Monterey, California in September 1999. This workshop investigated the effects of environmental variability, i.e. range, depth, and azimuthal variability on

acoustic signal propagation, the accuracy of the applied propagation models, and considered some limited signal processing of the modeled acoustic fields. In this section of the report we give results for acoustic propagation in a soliton environment. In physics, a soliton is a self-reinforcing solitary wave (a wave packet or pulse) that maintains its shape while it travels at constant speed. Solitons are caused by a delicate balance between nonlinear and dispersive effects in the medium. Dispersive effects refer to a relationship between the frequency and the speed of the waves in the medium.

The background sound speed profile is defined by

$$\begin{aligned} c(z) &= 1515 + 0.016z && \text{for } z \leq 26 \\ c(z) &= c_0(1 + a(e^{-b} + b - 1)) && \text{for } z \geq 26 \end{aligned} \tag{6.1}$$

where $c_0 = 1490m/s$, $a = 0.25$, $b = (z - z_{axis})/500$, and $z_{axis} = 200m$

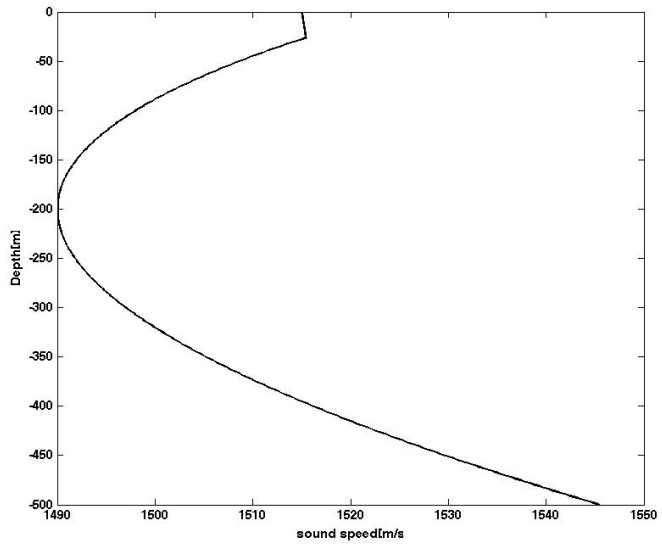

Figure 6.1: Background sound speed profile for the SWAM99 soliton study. Note that in the SWAM99 study, a flat bottom is set at a depth of 200m.

In the SWAM99 benchmark, a flat bottom is assumed at 200m depth, thus making it a shallow water problem.

A soliton perturbation to this background speed profile is given as:

$$dc(z, r) = C\frac{z}{B}e^{z/B}\sum_{i=1}^{6} A_i\big(\text{sech}(\frac{R_i - r}{D_i})\big)^2 \tag{6.2}$$

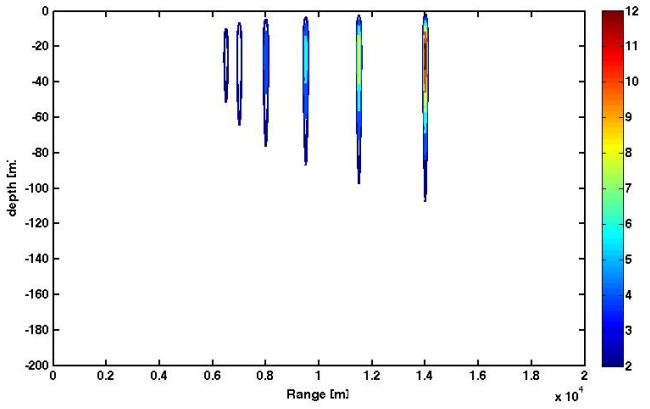

Figure 6.2: The added soliton configuration, max speed perturbation by solitons (rightmost) set to 12.5 m/s. Water depth and range: 200m and 20km.

where

$$\text{for } i = 1 \cdots 6 : A_i = 10e{-}0.3(i-1), \text{ and } D_i = \sqrt{34300/A_i} \tag{6.3}$$

$R_1 = 1400m$, and for $i = 2 \cdots 6 : R_i = R_{i-1} - 500(7-i)$,
$B = 25m$. C defines the maximum speed perturbation. $C = 3.4$ gives $dc = 12.2m/s$ while $C = 5$ gives $dc = 18.5m/s$.

This then constitutes a line of solitons spaced unevenly along the lower delimeter of the upper mixing zone of figure 6.1 above. The scenario is based on the study by Tielbürger et al. [11]. Analyzing the equation above, and the figure below show that the strength of the solitons vary. They increase in strength, *i.e.* velocity perturbation with increasing range. Figure 6.3 shows a ray tracing situation for the background sound speed distribution, that is, the one without solitons. 11 rays are emitted between $\pm 5^\circ$ The source is placed at 35m depth. We see rays bouncing off the bottom, some using the whole water volume as propagation channel, while others use the channel bounded by the bottom and the inflection point at 26m depth. In figure 6.4 we have plotted the number of rays crossing 50m long "bins" along the 35m depth receiver line. This can be regarded as a rough incoherent transmission loss measure with no adjustment for geometric losses with distance. The main reason for such plots is for comparisons to similar plots for the scenario including solitons. The plot shows a fairly repetitive pattern in the distribution with high levels around the upper turning points of the rays using the lower transmission channel.

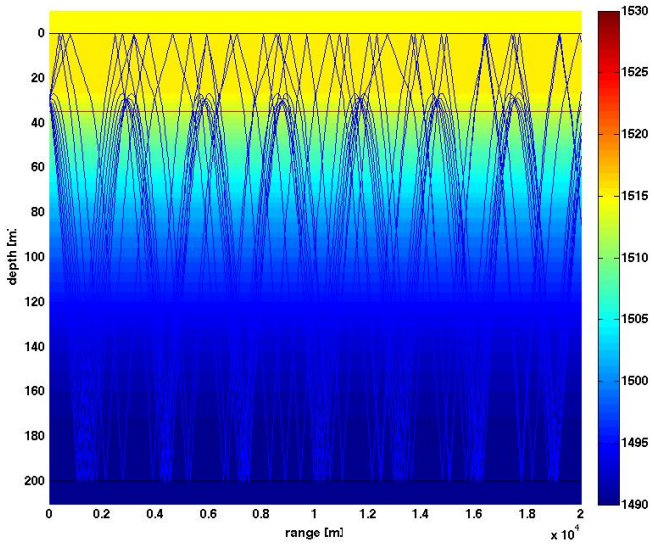

Figure 6.3: Rays emitted between ± 5 degrees, source depth = 30m, receiver depth =35m, scenario without solitons. Water depth and range: 200m and 20km.

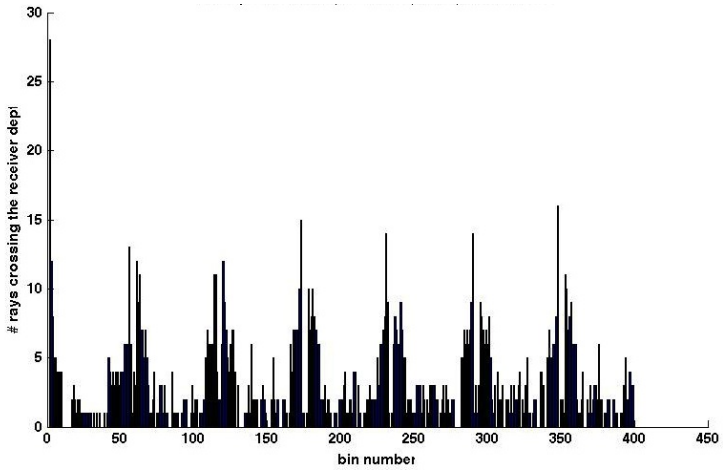

Figure 6.4: Rays emitted between $\pm 5^\circ$ every 0.1°. Number of rays crossing 50m long bins from zero to 20000m range, receiver depth = 35m.

Figures 6.5 and 6.6 of this section show similar plots when the solitons are included. A C factor of 5 is chosen corresponding to a maximum sound speed perturbation of 18.4 m/s. It is seen that the solitons disturb the ray transmission by deflecting the rays to new directions. The ”bin” diagram also shows that the crossings are less periodic beyond the solitons and shows sections of higher levels than in figure 6.4.

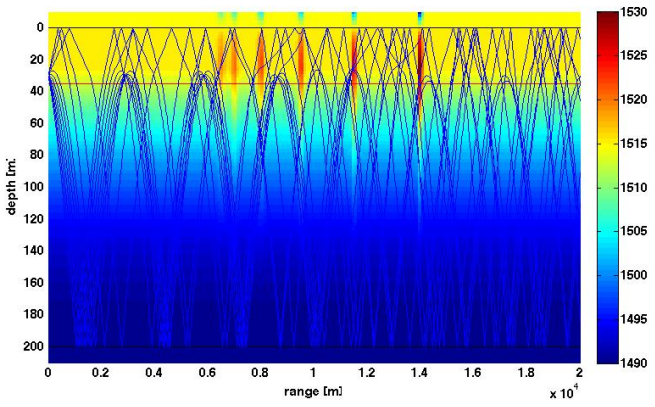

Figure 6.5: Rays emitted between ± 5 degrees, source depth =30m, receiver depth =35m, scenario with solitons. Water depth and range: 200m and 20km.

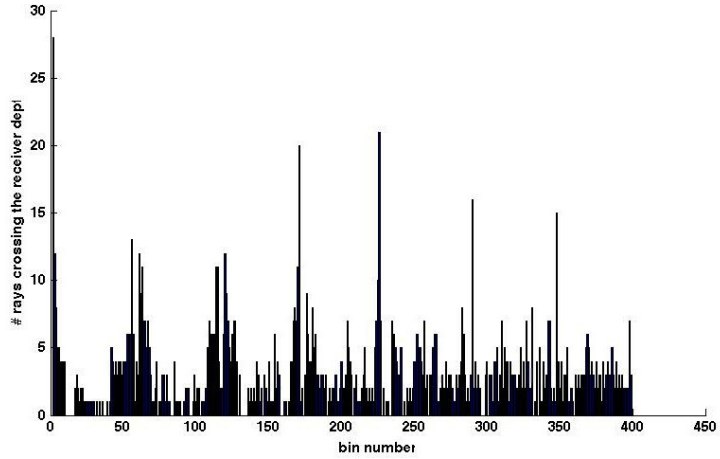

Figure 6.6: Rays emitted between $\pm 5^\circ$ every $.1^\circ$. Number of rays crossing 50m long bins from zero to 20000m range, receiver depth = 35m

The following figures pertain to a situation where the upper region has been used as a transmission channel. By placing the source at 10m depth and limiting the ray fan to $\pm 1^\circ$ the rays will not escape the upper channel in the undisturbed case. Only 11 rays are drawn for legibility of the figures. Adding a set of solitons using C=5 in the functional description makes a large part of the rays escape the upper channel and consequently disturbs the transmission possibilities of the channel.

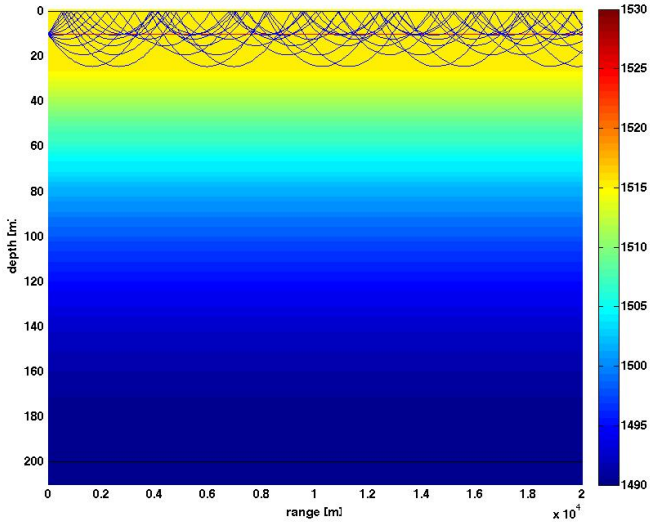

Figure 6.7: Rays emitted between $\pm 1^\circ$, source depth =10m. scenario without solitons. Water depth and range: 200m and 20km.

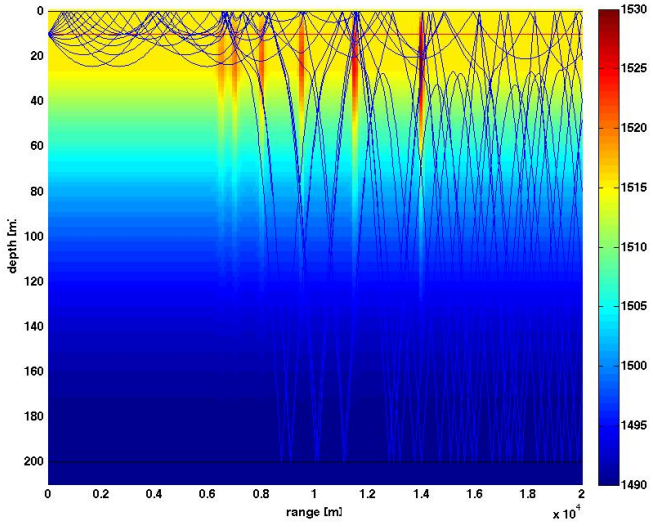

Figure 6.8: Rays emitted between $\pm 1^\circ$, source depth =10m, scenario with solitons. Water depth and range: 200m and 20km.

Figures 6.9 and 6.10 further indicate the influence of soliton strength. In figure 6.9 we have used a C factor of 0.05 corresponding to a velocity perturbation of only 1.8 m/s, while in figure 6.10, the C factor is 3.4 corresponding to a velocity perturbation of 12.5m/s.

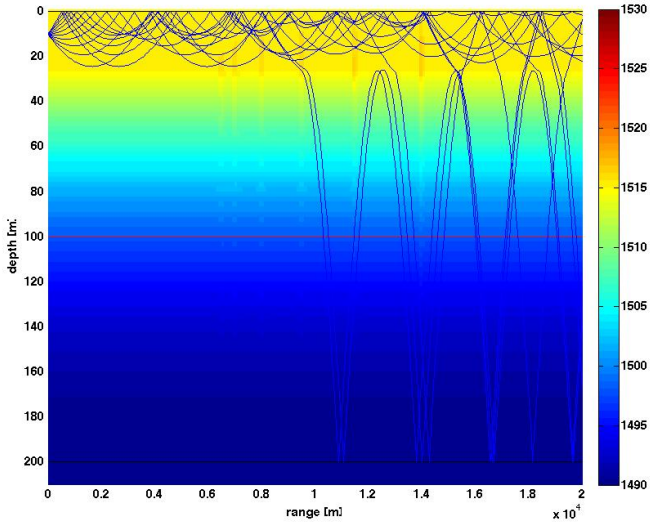

Figure 6.9: Rays emitted between $\pm 1^\circ$, source depth =10m. C factor 0.05. Water depth and range: 200m and 20km.

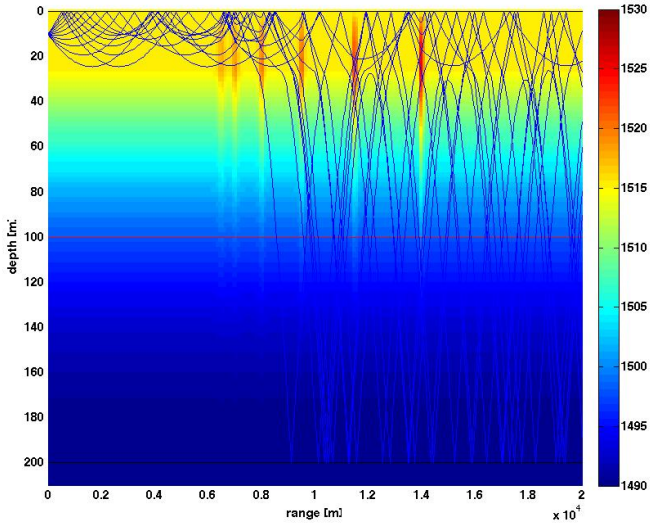

Figure 6.10: Rays emitted between $\pm 1^\circ$, source depth =10m, C factor 3.4. Water depth and range: 200m and 20km.

7 Conclusions

In section 3 of this report were described how the two raytracing programs Lybin and Ray5 can be used to model acoustic propagation in range dependent sound speed profile environments. The environment in question is one investigated by FFI in an earlier measurement campaign. The main purpose of this investigation was to find out if Lybin, which includes range dependence in an approximate way by defining range ”blocks” of constant profiles, would give similar results as Ray5, which is purposely written to handle range dependent environments. It was found that provided the data set describing the sound speed variation is properly smoothed, the two programs produce very similar ray traces. This gives us confidence in using Lybin for range dependent sound speed environments.

An investigation on the number of range blocks needed when preparing Lybin for sound propagation calculations showed that for the measured sound speed environment, the number of blocks is determined by the number of independent sound speed profiles measured. Finer block divisions in regions where the sound speed profiles are given by interpolations between the original independently measured ones, will only to a small extent influence the transmission loss.

An investigation was also done on the number of blocks needed for an environment characterized by a transition zone between two water volumes having different sound speed profiles. It was found that the necessary number was determined by a block width being roughly of the same length as the transition zone between the water volumes.

The Ray5 program was further used to study sound propagation in somewhat idealized range dependent situations, involving oceanographic features presented in the open literature. They were all considered deterministic, random fluctuations that certainly occur in real life are not included. The geometries consisted of: 1) wave propagation through an internal oceanographic wave, 2) long range propagation in the region of a hot center vortex, and 3) sound propagation in the region of an internal wave broken up into 4 solitary sound speed disturbances.

Ray diagrams and transmission loss studies showed that an internal wave, and also a set of solitons, will have a strong effect on sound transmission through such features *i.e.* focusing of sound to certain regions and, in the case of solitons close to a transmission channel, making sound energy propagate away from the channel.

It was also found that in the case of sound propagation in the region of a hot core vortex, Ray5 would give results close to results presented in the literature obtained by other methods.

References

[1] Marie Darrieus. Personal project in laboratory: Sound propagation in regions having variable oceanography. *NTNU/ENSTA*, 2008.

[2] B. Fujii, Y. Kagawa, T. Tsuchiya, and K. Fujioka. Discrete Huygens' model approach to sound wave propagation. *Journal of Sound and Vibration*, 218(3):419–444, 1998.

[3] A. Gangopadhyay and A.R. Robinson. Feature-oriented regional modeling of oceanic fronts. *Dynamics of Atmospheres and Oceans*, 36:201 – 232, 2002.

[4] Even Martin Grytå. Lydutbredelse i havområder med avstandsavhengig oseanografi, master's thesis. *NTNU*, 2009.

[5] Lincoln Baxter II and Marshall H. Orr. Fluctuations in sound transmission through internal waves associated with the thermocline: A computer model for acoustic transmission through sound velocity fields calculated from thermistor chain, ctd, xbt, and acoustic backscattering. *Journal of the Acoustical Society of America*, 71:61–66, 1982.

[6] Finn B. Jensen, William A. Kuperman, Michael B. Porter, and Henrik Schmidt. *Computational ocean acoustics*. Springer verlag New York, 2000.

[7] Owen S. Lee. Effect of an internal wave on sound in the ocean. *Journal of the Acoustical Society of America*, 33:677–681, 1961.

[8] Håvar Slåttrem Olsen. Lydutbredelse i havområder med avvstandsavhengig oseanografi, master's thesis. *NTNU*, 2008.

[9] Håvar Slåttrem Olsen. Lydutbredelse i havområder med avvstandsavhengig oseanografi, 5th year project. *NTNU*, 2007.

[10] M.B. Porter and H. P. Bucker. Gaussian beam tracing for computing ocean acoustic fields. *Journal of the Acoustical Society of America*, 82:1349 – 1359, 1987.

[11] Dirk Tielbürger, Steven Finette, and Stephen Wolf. Acoustic propagation through an internal wave field in a shallow water waveguide. *Journal of the Acoustical Society of America*, 101:789 – 808, 1997.